Analysis of the UV ozone-treated SnO_2 electron transporting layer in planar perovskite solar cells for high performance and reduced hysteresis

P. F. Mendez,[a], [b] Salim K.M Muhammamed,[b] Eva M. Barea,[b] Sofia Masi, [b] and Iván Mora-Seró* [b]*

[a] Facultad de Ciencias Químico Biológicas, Universidad Autónoma de Sinaloa, Cd. Universitaria, Av. de las Américas y Josefa Ortiz S/N, 80000, Culiacán, Sinaloa, México

[b] Institute of Advanced Materials (INAM), Universitat Jaume I, Av. Sos Baynat, s/n, 12071 Castelló, Spain

Corresponding Authors: masi@uji.es, sero@uji.es

Abstract

Tin oxide (SnO_2) is widely used as electron transporting layer (ETL) in perovskite solar cells (PSCs) because its good transparency, band alignment to perovskite and stability. The interface between the ETL and the perovskite in the PSCs affects the charge extraction process and may influence the optoelectronic properties. Surface treatment of SnO_2, such as the UV-ozone (UVO) treatment has been shown to enhance the efficiency and reduce the light soaking effect of the PSCs. Herein, we report the success in control and suppressing hysteresis reaching as highest photoconversion efficiency 19.4% with negligible hysteresis for the devices growth on 60 minutes UVO treated SnO_2. The wettability of treated SnO_2 is well-matched with the polar solvent of the perovskite solution, leading to complete coverage of the substrate, although the treatment does not affect the morphology and the crystallinity of the perovskite thin films. Impedance spectroscopy measurements analysis, clearly indicate the decrease of recombination rate after UVO treatment and the reduction of low frequency capacitance causing a reduction of current-potential curve hysteresis.

1. Introduction

The power-conversion efficiencies of perovskite solar cells (PSC) overcomes a power conversion efficiency (PCE) of 24%.[1] In a typical perovskite solar cell either with or without mesoporous scaffold, an absorber layer is sandwiched between electrode-modified layers including the electron and hole transport layers, ETLs and HTLs, respectively, acting as charge selective contacts. Currently, a lot of n-type metal oxides such as TiO_2,[2] SnO_2,[3] ZnO,[4] WO_3,[5] In_2O_3,[6] $SrTiO_3$,[7] and Nb_2O_5,[8] have been investigated as ETLs in PSCs architectures. Among them, SnO_2 is the most common ETL in PSCs, especially in most of highly efficient PSCs,[9] including current published record device (steady-state PCE of 23.32%).[1a] Furthermore, for fabrication of SnO_2 ETLs a low temperature process is especially favorable, due to its degradation tendency at high temperature[10] with the advantages of low cost, easy preparation, and outstanding performance in PSCs.[9] Moreover SnO_2 shows an excellent optical transparency in the visible range and better electric properties, band alignment to perovskite,[11] and stability,[12] making it a

promising candidate for commercialization of perovskite photovoltaic technology,[13] in planar configuration that present significant advantages in terms of cost and environmental impacts respect the mesoporous configuration.[14]

The implementation of SnO_2 as ETL was either demonstrated in dye-sensitized solar cells (DSSCs),[15] or in PSCs [11] and an impressive certified record efficiency of 20.9%, was achieved with SnO_2 nanoparticle in a planar architecture.[16] Currently, the explored techniques for the preparation of SnO_2 ETLs have been over ten different methods, [3, 9, 11, 17] and the most widely used are sol–gel technique with a spin-coating process.[18] Moreover a broad range of comparative studies[19] show the performance of SnO_2 PSCs is higher after surface modification made with several methods, that can be summarized in three main categories: surface treatments (with $TiCl_4$[20] or UV ozone (UVO) treatments[21]), SnO_2-based bilayer (fullerene[9] or TiO_2 interlayer[22]) and elemental doping[23]. The UVO treatment in particular is used as low temperature in situ sintering of SnO_2[24] to facilitate the deposition on flexible substrates or as surface treatment for removing organic residual. In this broad context we found that fresh-prepared SnO_2 films used in PSCs reported in literatures are UV-treated for few minutes before the perovskite deposition. [11, 17b] However, only few works reports the performances without UVO treatment as in the Wang et al. study, in which the PCE dramatically increases from 0.9% to 18%[21] or in the work of Bu at el., in which they demonstrate that a proper thermal-UVO treatment has some benefits for the charge transport, leading to an hysteresis free solar cells.[25] Here we investigate systematically the effect on PSCs efficiency of UVO treated-SnO_2 layer, deposited from a commercial colloidal solution, at different exposure time. By impedance spectroscopy (IS) we explain the reason why the treatment is so effective, highlighting the potential of SnO_2 without any significant surface modification towards an outstanding PCE of 19.4%. In details the treatment of SnO_2 affects the performance of PSCs in a number of ways: i) to improve wettability of the active absorber layer, ii) to reduce the hysteresis of the devices and iii) to passivate the surface states with the reduction of recombination and the increase of the open circuit-voltage.

2. Results and discussion

Several surface modification techniques have been developed to improve wetting, adhesion, and compatibility of ETL-perovskite interface. Surface modification methods, such as plasma treatment or ultraviolet-ozone (UVO) are employed to introduce functional groups on surfaces with minimal alteration of bulk properties, resulting in improved perovskite deposition, spreading, and crystal growth.[26] UVO treatment has many advantages over other methods for surface modification of ETL because it is cost effective and involves only simple apparatus with no requirement of vacuum systems. Ozonation treatment with UV light can also easily be carried out in various gasses, solvents and solutions at room temperature and this method is suitable for heat unstable materials such as organic substrates (Poly(3,4-ethylenedioxythiophene)-poly(styrenesulfonate) PEDOT:PSS, Poly[N,N'-bis(4-butylphenyl)-N,N'-

bis(phenyl)- benzidine] p-TPD or Poly(triaryl amine) PTAA), common implemented in the inverted solar cell architectures.[26]

The reactive oxygen radicals, produced by UVO attack, lead a partial surface hydroxylation of the tin-oxygen bounds (Sn–O) and substitute them with tin-hydroxide (Sn–OH), see scheme in Figure 1a. The enhancement of hydrophilicity of the surface after the UVO treatment is confirmed using water contact angle measurement, which decreased from 80° to 17° (Figure 1a) after one hour of UVO treatment. This effect is reported in literature and only few minutes of treatments are enough to improve the wettability of the perovskite solution.[26] The surface morphology of the SnO_2 layer is completely uniform, as the Scanning Electron Microscopy (SEM) images show in Figure 1b and the UVO treatment does not affect the crystallinity, as the X-Ray Diffraction (XRD) patterns before and after the treatment are similar (Figure 1c). The SnO_2 layer before and after the UVO treatment shows four peaks located at 2θ = 26.6°, 33.8°, 37.8° and 51.5° correspond, respectively, to the (110), (101), (200) and (211) crystalline planes of SnO_2 with tetragonal cassiterite structure.[27]

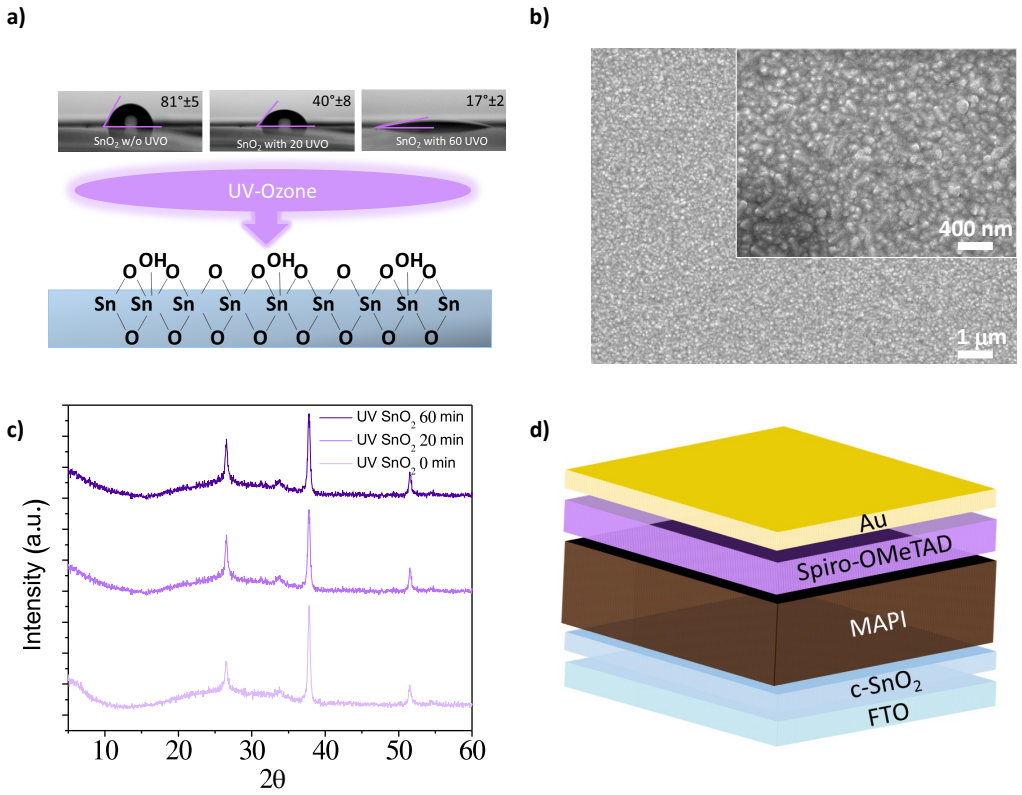

Figure 1. a) Contact angles of FTO/SnO_2 substrates without treatment and with 20 min and 60 min of UVO treatment; a schematic representation of the surface hydroxylation after UVO treatment is reported; b) SEM top view of SnO_2 layer; the scale bar is 1 µm and the inset is a zoom with a scale bar of 400 nm; c) XRD pattern of the SnO_2 layer with and without UVO treatments. d) Sketch of the perovskite solar cells based on glass/FTO/SnO_2 (40 nm)/Perovskite (250 nm)/spiro-OMeTAD (200 nm)/Au.

In order to quantify the effect of UVO treatment in the interfacial properties and ultimately in the final PSC performance, we fabricated and characterized PSCs with planar architecture as it is shown in Figure 1d (Glass/FTO/SnO_2/$MAPbI_3$/Spiro-OMeTAD/Au). The comparative analysis has been made between solar cells with untreated SnO_2, (UV-SnO_2 0 min) even the coverage is not complete (Figure S1), and with 20 min (UV-SnO_2 20 min) and 60 min of UVO treatment (UV-SnO_2 60 min). Our results are summarized in Figure 2 and Table 1. Immediate observations that can be made are: (i) the average power conversion efficiency (PCE) increases with the treatment time (Table 1), in the case of the champion cells PCE increases from 16.1% for devices prepared without UVO treatment to 17.7% for UVO-20 min SnO_2 based devices to 19.4% for cells prepared with 60 min UVO treatment; (ii) all solar cell parameters, the open-circuit voltage (V_{oc}), the photocurrent (J_{sc}) and the fill factor (FF), increase with the UVO exposure time (Figure 2) and (iii) devices where UVO is used display a significantly reduced hysteresis (Figure 3). This superior photovoltaic performance that is observed for the devices from treated substrates, on the one hand, can be attributed to the formation of a very uniform perovskite layer caused by the improved wettability (Figure 1a). This can have a few likely benefits: such a uniform layers can prevent undesirable recombination processes that occur through direct contact between SnO_2 and a hole-transporting layer; it, thus, assists in increasing the charge collection efficiency

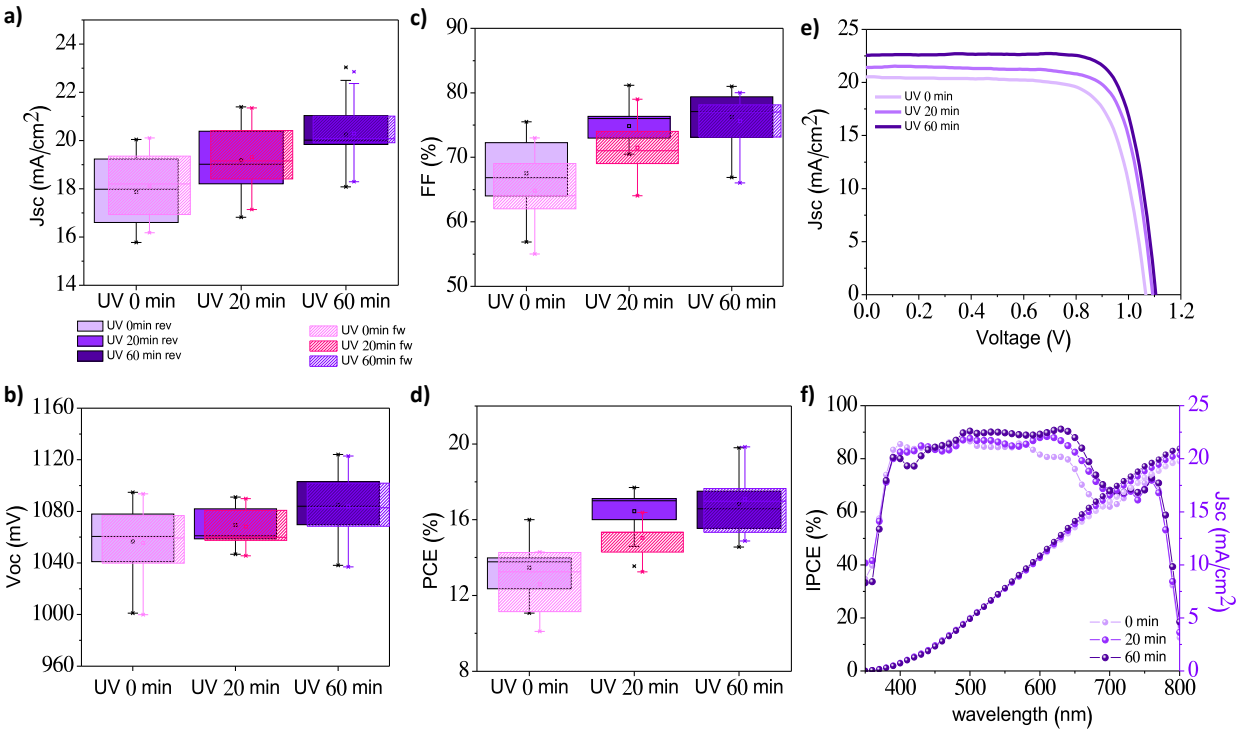

Figure 2. Statistical analysis of forward potential scan (fw) and reverse potential scan (rev) results of a) Jsc, b) Voc, c) FF, d) PCE of the perovskite solar cells fabricated without UVO treatment, and with UVO treatment of 20 min and 60 min. The data from 40 cells were statistically analyzed; e) J-V curves of the best performance perovskite

solar cells recorded at reverse scan; f) IPCE spectra and integrated photocurrent of the best solar cells without and with the UVO treatment.

Table 1. Figures of merits, J_{sc}, FF, V_{oc}, PCE, expressed as mean and standard deviation, in forward and reverse scan and the best PCE of PSCs with UVO-SnO_2 (20 min and 60 min) and without treatment.

UVO time	J_{sc} (mA/cm²)	FF	V_{oc} (mV)	PCE (%)	Best PCE (%)
0 min rev	17.9 ± 1.4	67.5 ± 5.1	1056 ± 26	13.4 ± 1.3	16.1
0 min fw	17.8 ± 1.4	64.8 ± 4.6	1056 ± 26	12.4 ± 1.4	13.9
20 min rev	19.2 ± 1.5	74.8 ± 2.8	1069 ± 13	16.7 ± 1.6	17.7
20 min fw	19.2 ± 1.5	71.5 ± 3.8	1069 ± 14	14.7 ± 0.7	14.7
60 min rev	20.4 ± 1.5	76.3 ± 3.5	1085 ± 21	17.2 ± 1.7	19.4
60 min fw	20.3 ± 1.5	75.5 ± 3.6	1085 ± 21	16.7 ± 1.6	19.2

and the FF. On the other hand, improving the interfaces of the active layer has a direct impact on the V_{oc}, resulting also in an average improvement of the PCE (Figure 2). It is worth to note that with 10 min or 45 min of the UVO treatment the performances approaching the one of the 20 min and 60 min respectively, finally reaching a plateau (Figure S2). This is a very clear evidence of how the effect of the UVO treatment can be distinguished before and after the 20 min: if the treatment is shorter than 20 min we only can improve the wettability of the SnO_2 with a good quality perovskite layer on the top, but if we maximize the treatment up to 60 min the positive effect on the charge collection and extraction at the interface is undiscussed, as we proved with the reduction of the hysteresis.

Concerning the device performance, the PSC efficiency is mainly related to the active layer quality, morphology and crystallinity. It is commonly little change in morphology can lead to profound difference in the transport properties. A systematical SEM analysis, absorbance and

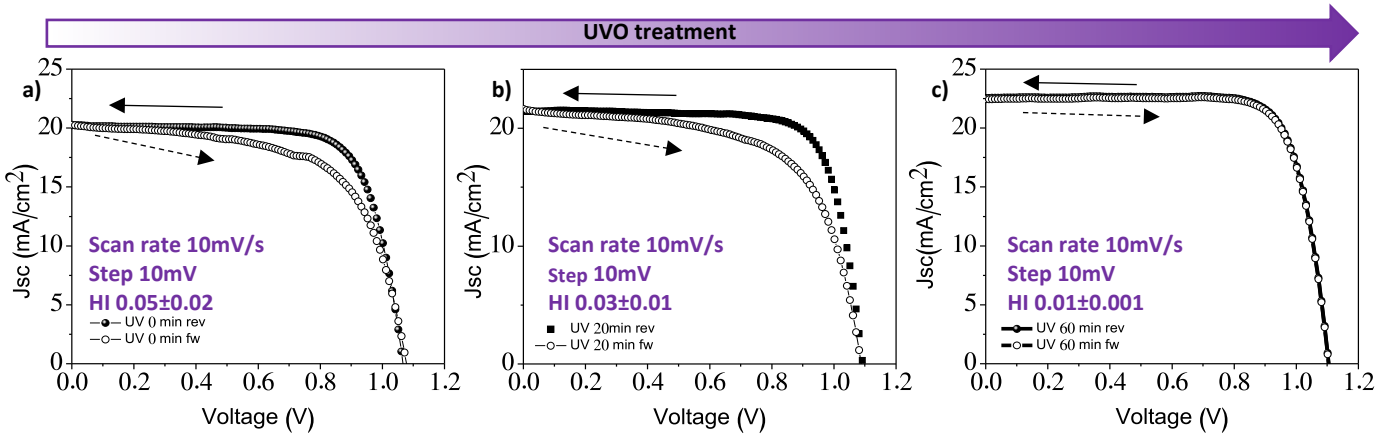

Figure 3. Hysteresis effect of perovskite solar cell a) without, b) with 20 min and c) with 60 min of UVO treatment. Inset with the statistic of the hysteresis index (HI) calculated as reported in ref. [28] HI is an appropriated quantitative parameter to compare hysteresis among samples measured used the same protocol.

XRD measurements are thus a must to correlate the effect of the treatment with the final performances, however the morphology does not significantly change with the treatment (Figure S3a) and all the samples showed the same thickness, as it is possible to see in the cross section images (Figure S3b) and the same absorbance (Figure S3c). Likewise it can be observed in the absorbance spectra a peak onset around 780 nm with a band gap of 1.59 eV (Figure S3c). All these evidence are in accordance with the small deviation among samples observed for the J_{sc} (Figure 2a). We present also the incident photon-to-electron conversion efficiency (IPCE) spectrum of the best PSCs at each condition in Figure 2f. The integrated current densities derived from the IPCE spectrum (Figure 2f) are 22.3 mA/cm^2, 21.1 mA/cm^2 and 20.2 mA/cm^2, in good agreement with the J_{SC} value obtained from the *J–V* curves, excluding significant spectral mismatch between our simulator and the AM 1.5G solar source. Moreover no significant changes in the position of diffraction peaks were observed as effect of UVO treatment, therefore, the treatment does not modify the crystalline structure of the deposited perovskite (Figure S1d). The XRD spectra show the presence of six main peak at 14.12°, 20.04°, 24.52°, 28.48°, 31.92°, and 40.72°, which correspond to the (110), (112), (202), (220), (310) and (224) planes for the perovskite $MAPI_3$. It is worth to note that in the procedure for the preparation of the perovskite film (see Experimental section in Supporting Information) we use an annealing temperature of 130 °C for 10 minutes, and the typical precursor peak of the lead iodide at 12,5° is not observed, confirming that these conditions are not enough to decompose the perovskite. We seem also to learn about the solution requirements that lead to optimum device performance. For instance, we find that pristine $MAPbI_3$ in pure dimethyl sulfoxide (DMSO) annealed for 10 min at 130 °C displays a higher fill factor than the $MAPbI_3$ in a mixture of dimethylformamide (DMF) and DMSO (DMF:DMSO 10:1)[29] at the same temperature (Figure S4). These findings reflect the homogeneity of the prepared perovskites, but also indicates that the UVO treatment does not modify the structural properties of the active perovskite layer.

Consequently, the improvements in photovoltaic parameters can be related to a better quality of the interface SnO_2/perovskite. Photoluminescence (PL) of perovskite layers deposited on glass with or without SnO_2, and protected from moisture by the poly(methyl methacrylate) (PMMA) inert polymer,[30] was analyzed. In order to rule out differences among the SnO_2 in their capability of efficient extraction of the charge from the perovskite layer, time-resolved (TRPL) radiative emission from the active layer in the presence or absence of the charge extracting layers are assessed (Figure 4a). The pristine material shows long PL decays confirming low electronic trap densities and balanced carriers transport.[31] In comparison, the decays associated with this emission when the perovskite active layer was coupled to the SnO_2 are significantly faster, especially when the UVO treatment is performed , suggesting more efficient electron extraction process when the SnO_2 is treated for 60 minutes. (Table S1)

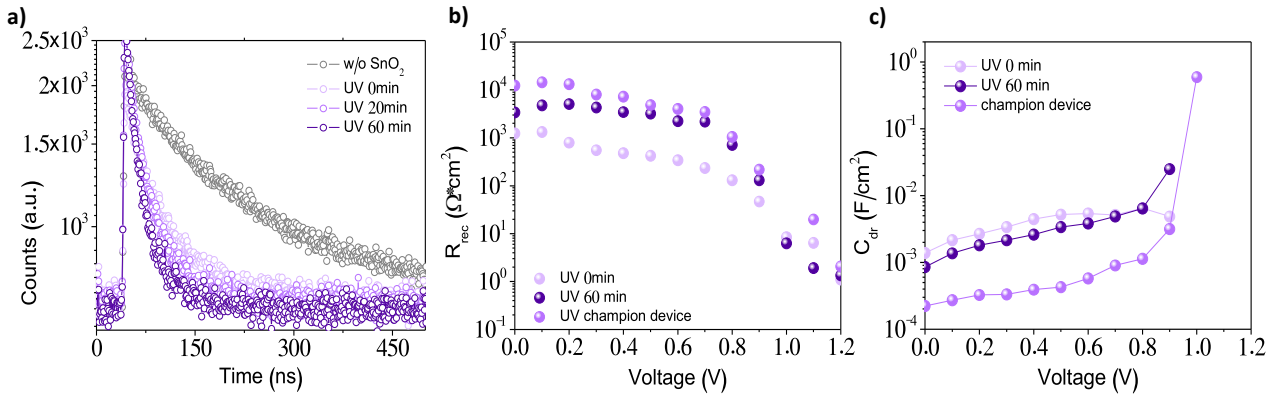

Figure 4. a) Time-resolved PL decay of the corresponding perovskite films, deposited either on glass, or on SnO_2; b) Plot of recombination resistance (R_{rec}) vs. applied voltage and c) plot of the capacitance (C_{dr}) vs. applied voltage of devices based on SnO_2 without treatment, with 60 min UVO treatment and of the champion device.

Impedance spectroscopy (IS) is another effective tool to provide insight into the electronic transport processes involved in the devices. IS measurements are performed on complete, planar PSCs with various UVO treatments to evaluate variations in V_{oc}, FF, PCE. Measurements were carried out under Xenon lamp (intensity 100mW/cm²) illumination over a wide range of applied voltages and frequencies (from 0 up to Voc and from 1MHz to 0.1 Hz).[32] The fitting has been performed using the equivalent circuits discussed elsewhere [33] and the recombination resistance (R_{rec}) has been obtained by addition of the resistances of high frequency and low frequency (lf) semicircles obtained in the Nyquist plot,[33c] (Figure S5). From IS analysis, it is observed that the R_{rec} of average UVO 60 min SnO_2 treated PSC exhibit significantly higher recombination resistance than the UVO 0 min SnO_2 PSC over nearly the entire range of studied voltage bias, indicating that the non-radiative recombination rate is significantly lower (Figure 4b). These increase is even more clear in the case of champion device with 60 min UVO treatment, pointing a reduction of the recombination rate as the main effect of treatment, that is attributed to the different interaction at the perovskite/SnO_2 interface. The increase R_{rec} indicates a decrease of the recombination rate with a consequent improvement of the V_{oc}., as it is in fact observed in Table 1 and Figure 2b. The lower surface recombination also contributes to the enhancement of photocurrent, [34] as observed in Figure 2a. In addition, the low frequency capacitance[35] observed for these samples, decreases after the UVO treatment especially for the champion cell. This observation confirms the trend relating the decrease of this capacitance with a decrease of the observed hysteresis.[36] There are different interpretations of the physical meaning of low frequency capacitance.[36a, 37] Despites the different interpretation it is commonly related with ion migration and interfacial effects.

Furthermore devices employing UVO 60 min SnO_2 exhibit substantially reduced hysteresis (Figure 3c), which is consistent with a larger surface area for electron injection, increasing the pathways for unhindered electron transfer. It hence appears that hysteresis comes out only when there exists poor electronic contact between the perovskite and the charge collection layer,[38] requiring the improved contact enabled by the more and more –OH functional groups, in line with the contact angle measurements, or less oxygen vacancies on the treated surfaces.[18, 39] In other words, the high hydrophilic surface of UVO 60 min SnO_2 and the better interaction between the perovskite and the substrate would enhance the electron transport from perovskite to SnO_2 ETL, leading to no significant charge accumulation, and consequently, the devices based on the UVO 60 min SnO_2 exhibit negligible hysteresis. (Figure 2d, 3c)[28]

All these facts confirm the positive effect of the UVO treatment, which influences the density and distribution of surface defects, believed to be oxygen vacancies and/or terminal hydroxyls groups, [40] playing a central role in the improvement of the interface SnO_2/perovskite quality and in the device performance by the reduction of the recombination rate.

3. Conclusions

The performances and hysteresis of PSCs was modified by adjusting the time of the UVO treatment on the tin oxide (SnO_2), used as ETL. With 60 minutes of UVO treatment we improved the solar cells efficiency as high as 19.4% with a hysteresis-free behavior. The outstanding properties of the treated samples are attributed to the good quality of the perovskite/SnO_2 interface including an improved wettability, enhanced recombination resistance, and the reduced oxygen vacancies. The treatment does not affect the structural properties of the perovskite layer deposited on top but leads an efficient charge collection at perovskite/ETL interface, in turn leading to higher solar cell parameters, FF, V_{oc} and J_{sc}, independently of the scan direction. The UVO treatment improves the contact charge selectivity, with a decrease of recombination rate of PSCs. These results highlight the potentiality of perovskite planar devices using low temperature deposition SnO_2 for the development of high performance devices with an appropriated treatment of the interfacial properties.

Acknowledgements

Financial support from the European Research Council (ERC) via Consolidator Grant (724424—No-LIMIT), Generalitat Valenciana project IDIFEDER/2018/012 and Universitat Jaume I (project SOLENPE UJI-B2016-05) are gratefully acknowledged. P.F Méndez thank Fundación Carolina and Universidad Autónoma de Sinaloa for short stay fellowship. Servei Central d'Instrumentació Científica (SCIC) from Universitat Jaume I is acknowledged for its help with SEM and XRD measurements.

References

[1] a) Q. Jiang, Y. Zhao, X. Zhang, X. Yang, Y. Chen, Z. Chu, Q. Ye, X. Li, Z. Yin, J. You, *Nature Photonics* **2019**, DOI: 10.1038/s41566-019-0398-2; b) www.nrel.gov/pv/assets/images/efficiency-chart.png.

[2] N. J. Jeon, J. H. Noh, Y. C. Kim, W. S. Yang, S. Ryu, S. I. Seok, *Nature Materials* **2014**, 13, 897.

[3] Q. Jiang, L. Zhang, H. Wang, X. Yang, J. Meng, H. Liu, Z. Yin, J. Wu, X. Zhang, J. You, *Nature Energy* **2016**, 2, 16177.

[4] J. Kim, G. Kim, T. K. Kim, S. Kwon, H. Back, J. Lee, S. H. Lee, H. Kang, K. Lee, *Journal of Materials Chemistry A* **2014**, 2, 17291.

[5] J. Zhang, C. Shi, J. Chen, Y. Wang, M. Li, *Journal of Solid State Chemistry* **2016**, 238, 223.

[6] M. Qin, J. Ma, W. Ke, P. Qin, H. Lei, H. Tao, X. Zheng, L. Xiong, Q. Liu, Z. Chen, J. Lu, G. Yang, G. Fang, *ACS Applied Materials & Interfaces* **2016**, 8, 8460.

[7] A. Bera, K. Wu, A. Sheikh, E. Alarousu, O. F. Mohammed, T. Wu, *The Journal of Physical Chemistry C* **2014**, 118, 28494.

[8] J. Saito, T. Oku, A. Suzuki, T. Akiyama, *AIP Conference Proceedings* **2016**, 1709, 020027.

[9] S.-H. Turren-Cruz, A. Hagfeldt, M. Saliba, *Science* **2018**, 362, 449.

[10] W. Ke, G. Fang, Q. Liu, L. Xiong, P. Qin, H. Tao, J. Wang, H. Lei, B. Li, J. Wan, G. Yang, Y. Yan, *Journal of the American Chemical Society* **2015**, 137, 6730.

[11] J. P. Correa Baena, L. Steier, W. Tress, M. Saliba, S. Neutzner, T. Matsui, F. Giordano, T. J. Jacobsson, A. R. Srimath Kandada, S. M. Zakeeruddin, A. Petrozza, A. Abate, M. K. Nazeeruddin, M. Grätzel, A. Hagfeldt, *Energy & Environmental Science* **2015**, 8, 2928.

[12] B. Roose, J.-P. C. Baena, K. C. Gödel, M. Graetzel, A. Hagfeldt, U. Steiner, A. Abate, *Nano Energy* **2016**, 30, 517.

[13] E. J. Yeom, S. S. Shin, W. S. Yang, S. J. Lee, W. Yin, D. Kim, J. H. Noh, T. K. Ahn, S. I. Seok, *Journal of Materials Chemistry A* **2017**, 5, 79.

[14] J.-A. Alberola-Borràs, R. Vidal, E. J. Juárez-Pérez, E. Mas-Marzá, A. Guerrero, I. Mora-Seró, *Solar Energy Materials and Solar Cells* **2018**, 179, 169.

[15] P. Tiwana, P. Docampo, M. B. Johnston, L. M. Herz, H. J. Snaith, *Energy & Environmental Science* **2012**, 5, 9566.

[16] Q. Jiang, Z. Chu, P. Wang, X. Yang, H. Liu, Y. Wang, Z. Yin, J. Wu, X. Zhang, J. You, *Advanced Materials* **2017**, 29, 1703852.

[17] a) M.-G. Kim, M. G. Kanatzidis, A. Facchetti, T. J. Marks, *Nature Materials* **2011**, 10, 382; b) J. Ma, X. Zheng, H. Lei, W. Ke, C. Chen, Z. Chen, G. Yang, G. Fang, *Solar RRL* **2017**, 1, 1700118; c) S. S. Shin, W. S. Yang, J. H. Noh, J. H. Suk, N. J. Jeon, J. H. Park, J. S. Kim, W. M. Seong, S. I. Seok, *Nature Communications* **2015**, 6, 7410.

[18] D. Yang, R. Yang, K. Wang, C. Wu, X. Zhu, J. Feng, X. Ren, G. Fang, S. Priya, S. Liu, *Nature Communications* **2018**, 9, 3239.

[19] a) L. Xiong, Y. Guo, J. Wen, H. Liu, G. Yang, P. Qin, G. Fang, *Advanced Functional Materials* **2018**, 28, 1802757; b) Q. Jiang, X. Zhang, J. You, *Small* **2018**, 14, 1801154.

[20] Y. Li, J. Zhu, Y. Huang, F. Liu, M. Lv, S. Chen, L. Hu, J. Tang, J. Yao, S. Dai, *RSC Advances* **2015**, 5, 28424.

[21] Q. Dong, Y. Shi, C. Zhang, Y. Wu, L. Wang, *Nano Energy* **2017**, 40, 336.

[22] M. M. Tavakoli, F. Giordano, S. M. Zakeeruddin, M. Grätzel, *Nano Letters* **2018**, 18, 2428.

[23] M. Park, J.-Y. Kim, H. J. Son, C.-H. Lee, S. S. Jang, M. J. Ko, *Nano Energy* **2016**, 26, 208.

[24] a) F. Li, M. Xu, X. Ma, L. Shen, L. Zhu, Y. Weng, G. Yue, F. Tan, C. Chen, *Nanoscale Research Letters* **2018**, 13, 216; b) L. Huang, X. Sun, C. Li, J. Xu, R. Xu, Y. Du, J. Ni, H. Cai, J. Li, Z. Hu, J. Zhang, *ACS Applied Materials & Interfaces* **2017**, 9, 21909.

[25] T. Bu, S. Shi, J. Li, Y. Liu, J. Shi, L. Chen, X. Liu, J. Qiu, Z. Ku, Y. Peng, J. Zhong, Y.-B. Cheng, F. Huang, *ACS Applied Materials & Interfaces* **2018**, 10, 14922.
[26] X. Xu, C. Ma, Y. Cheng, Y.-M. Xie, X. Yi, B. Gautam, S. Chen, H.-W. Li, C.-S. Lee, F. So, S.-W. Tsang, *Journal of Power Sources* **2017**, 360, 157.
[27] **International Center for Diffraction Data.**, Newtown Square: International Center for Diffraction Data; 1990.
[28] R. S. Sanchez, V. Gonzalez-Pedro, J.-W. Lee, N.-G. Park, Y. S. Kang, I. Mora-Sero, J. Bisquert, *J. Chem. Phys. Lett.* **2014**, 5, 2357.
[29] N. Ahn, D.-Y. Son, I.-H. Jang, S. M. Kang, M. Choi, N.-G. Park, *Journal of the American Chemical Society* **2015**, 137, 8696.
[30] J. M. Frost, K. T. Butler, F. Brivio, C. H. Hendon, M. van Schilfgaarde, A. Walsh, *Nano Letters* **2014**, 14, 2584.
[31] D. Yang, X. Zhou, R. Yang, Z. Yang, W. Yu, X. Wang, C. Li, S. Liu, R. P. H. Chang, *Energy & Environmental Science* **2016**, 9, 3071.
[32] D. Pitarch-Tena, T. T. Ngo, M. Vallés-Pelarda, T. Pauporté, I. Mora-Seró, *ACS Energy Letters* **2018**, 3, 1044.
[33] a) A. Guerrero, G. Garcia-Belmonte, I. Mora-Sero, J. Bisquert, Y. S. Kang, T. J. Jacobsson, J.-P. Correa-Baena, A. Hagfeldt, *The Journal of Physical Chemistry C* **2016**, 120, 8023; b) I. Zarazua, G. Han, P. P. Boix, S. Mhaisalkar, F. Fabregat-Santiago, I. Mora-Seró, J. Bisquert, G. Garcia-Belmonte, *The Journal of Physical Chemistry Letters* **2016**, 7, 5105; c) I. Zarazúa, S. Sidhik, T. Lopéz-Luke, D. Esparza, E. De la Rosa, J. Reyes-Gomez, I. Mora-Seró, G. Garcia-Belmonte, *The Journal of Physical Chemistry Letters* **2017**, 8, 6073.
[34] J. Idígoras, L. Contreras-Bernal, J. M. Cave, N. E. Courtier, Á. Barranco, A. Borras, J. R. Sánchez-Valencia, J. A. Anta, A. B. Walker, *Advanced Materials Interfaces* **2018**, 5, 1801076.
[35] E. J. Juarez-Perez, R. S. Sanchez, L. Badia, G. Garcia-Belmonte, Y. S. Kang, I. Mora-Sero, J. Bisquert, *J. Chem. Phys. Lett.* **2014**, 5, 2390.
[36] a) D. A. Jacobs, H. Shen, F. Pfeffer, J. Peng, T. P. White, F. J. Beck, K. R. Catchpole, *J. Appl. Phys.* **2018**, 124, 225702; b) H.-S. Kim, I.-H. Jang, N. Ahn, M. Choi, A. Guerrero, J. Bisquert, N.-G. Park, *J. Chem. Phys. Lett.* **2015**, 6, 4633.
[37] a) I. Zarazua, J. Bisquert, G. Garcia-Belmonte, *J. Chem. Phys. Lett.* **2016**, 7, 525; b) D. Moia, I. Gelmetti, P. Calado, W. Fisher, M. Stringer, O. Game, Y. Hu, P. Docampo, D. Lidzey, E. Palomares, J. Nelson, P. R. F. Barnes, *Energy & Environmental Science* **2019**, DOI: 10.1039/C8EE02362J.
[38] K. Wojciechowski, S. D. Stranks, A. Abate, G. Sadoughi, A. Sadhanala, N. Kopidakis, G. Rumbles, C.-Z. Li, R. H. Friend, A. K. Y. Jen, H. J. Snaith, *ACS Nano* **2014**, 8, 12701.
[39] F. Zhang, W. Ma, H. Guo, Y. Zhao, X. Shan, K. Jin, H. Tian, Q. Zhao, D. Yu, X. Lu, G. Lu, S. Meng, *Chemistry of Materials* **2016**, 28, 802.
[40] M. F. Mohamad Noh, N. A. Arzaee, J. Safaei, N. A. Mohamed, H. P. Kim, A. R. Mohd Yusoff, J. Jang, M. A. Mat Teridi, *Journal of Alloys and Compounds* **2019**, 773, 997.